Sensitivity analysis of the dynamic response of an electronic fuel injector regarding fuel properties and operating conditions

Nao Hu[1, 2, *], Jianguo Yang[1, 3], Peilin Zhou[2]

1. School of Energy and Power Engineering, Wuhan University of Technology, 430063, Wuhan, PRC;

2. Department of Naval Architecture, Ocean and Marine Engineering, University of Strathclyde, G4 0LZ, Glasgow, UK;

3. Key Laboratory of Marine Power Engineering &Technology, Ministry of Communications, 430063, Wuhan, PRC;

[*]. Corresponding author.

Abstract: The effects of fuel properties, such as its bulk modulus, density and viscosity, on the injector dynamic response (needle valve opening/closing delay and needle valve opening/closing time) were investigated individually. Firstly, an electronic fuel injector model was built and validated by injection rate and injection mass at three different rail pressures and three different activation times. Secondly, a DOE (design of experiment) model was built and the Uniform Latin Hypercube (ULH) design method was applied to study the influences of the fuel properties on the injector dynamic response from a statistical point of view. The effects of the fuel properties were compared by using a SS-ANOVA (smoothing spline analysis of variance) method at both a low and a high rail pressure. The bulk modulus was found to play a dominant role in influencing the valve opening/closing delay at the low rail pressure. However, at the high rail pressure, the effects of the viscosity are prominent, while the effects

[*] Email: nao.hu.0128@gmail.com (N. Hu)

of the bulk modulus and the density are negligible. Additionally, how these fuel properties affect the dynamic response were reported by RSM (Response Surface Method) function charts, and the details of the pressure differences and needle valve movements were also disclosed.

Key words: electronic fuel injector; fuel properties; dynamic response; DOE

Nomenclature

1D	one dimensional	ULH	Uniform Latin Hypercube
AC	accumulation chamber	v	pressure wave propagation speed
Ab_Visc	absolute viscosity		
B	bulk modulus	*Greek symbols*	
Bulk_M	bulk modulus	μ	absolute viscosity
CC	control chamber	ρ	density
C_f	friction coefficient	τ	delay
D	pipe diameter		
Dens	density	*Units*	
DOE	design of experiments	cP	centipoise
HPCR	high pressure common rail	K	Kelvin
L	pipe length	kg/mm^3	kilograms per cubic millimetre
n	levels	m	metre
NN	neural networks	mg/st	milligram per stroke
R_e	Reynolds number	MPa	mega Pascal
RSM	response surface method	ms	millisecond
s	field	N	Newton
SS-ANOVA	smoothing spline analysis of variance algorithm	Pa·s	Pascal second
T	time constant		

1. Introduction

Electronic fuel injectors play an indispensable role in HPCR fuel injection systems and interest numerous researchers to improve their performance. A lot of work has been undertaken in the nozzle area, such as the nozzle structure types [1-3], the hole numbers and arrangements [4-7] and the internal cavitation [8-11] of orifices. They have been thoroughly studied because they have a direct effect on the fuel injection and atomisation. The spray characteristics [12-14], the penetration [15-17] and the lift-off length [18,19] have also been investigated by experiment or simulation in many studies. With the continual focus on the emissions of diesel engines, the use of different alternative fuels has come into the sight of researchers [20]. The differences in fuels lie in their properties [21], such as the density, viscosity and bulk modulus. Fuel properties significantly affect the spray characteristics of a fuel injector, as were studied by Dernotte et al. [22] and Payri et al. [23]. In addition, fuel properties change in vast ranges of different pressures and temperatures, as were revealed by Salvador et al. [24] and Desantes et al. [25].

The multi-injection performance of a solenoid injector was evaluated by Salvador et al. [26] by using a standard diesel fuel and a biodiesel fuel. The biodiesel fuel was identified as have a larger valve opening delay and valve opening time due to it have a larger viscosity. This implies that the fuel properties may have an effect on the dynamic response of a fuel injector. However, to date, only a few studies have found considered the effects of fuel properties on the dynamic response of electronic fuel injectors. Han et al. [27] experimentally investigated the injection process of three fatty acid esters on an HPCR system. He pointed out that fatty acid esters have larger injection delays and smoother rising slopes of the injection rate than diesel fuel. They also indicated that a reduced injection delay, along with a prolonged injection duration, was seen at increased rail pressures. Salvador et al. [28] experimentally investigated the impact of

fuel temperature on the injection dynamics (stationary mass flow rate, injection delay, and valve opening/closing slope of the mass flow rate) of a ballistic injector, with special attention paid to the needle valve opening and closing stages. They indicated that the temperature had a huge influence on the valve opening delay. In a further study to extend insights into the injector dynamics, Payri et al. [29] developed a one-dimensional model and paid special attentions to the pressure drop in the control chamber, the viscous friction and the needle lifts. These studies investigated the injection dynamic with different fuels or different fuel temperatures and pressures, yet the impact of each fuel property on the injector dynamic response is still not clearly identified. Boudy et al. [30] investigated the influence of the properties of a biodiesel fuel on the injection process; in this study, the fuel density, bulk modulus and absolute viscosity were examined individually in both single- and triple-injection situations. He pointed out that density is one of the most influential fuel properties on the injection process. Han et al. [31] investigated the isolated effect of the fuel density, viscosity and bulk modulus on the injection mass and pressure propagation waves under split injection strategy conditions. They indicated that the fuel density and bulk modulus have a larger impact than the viscosity on the injection mass and pressure propagation. However, in these studies, the fuel properties varied only slightly, and the dynamic response, such as the needle valve opening/closing delay and opening/closing time, was not in their interests.

One-dimensional (1D) models are efficient and practical for predicting the performance of electronic fuel injectors, and have been adopted by many studies. For example, a 1D model of a solenoid-driven common rail ballistic injector was built by Payri et al. [32] to study the influences of the inlet fuel temperature on the injection rate. Ando et al. [33] investigated the magnetic aftereffect on the dynamic response of a fuel injector by building a simple and high accurate 1D simulation model. They indicated that a significant delay was caused by a lower

maximum activation current, which generated a smaller magnetic force than a higher maximum activation current. Another 1D model was built by Seykens et al. [34] to investigate the elasticity and nonlinearities of the injector needle valve. Additionally, 1D hydraulic models were also established by Han et al. [31] and Rahim et al. [35]. The detailed modelling of fuel injectors was demonstrated by Bianchi et al. [36], Payri et al. [32, 37] and Salvador et al. [38].

In this paper, the effects of three fuel properties (the fuel density, bulk modulus and absolute viscosity) on the valve opening/closing delay and the valve opening/closing time were carefully investigated. Firstly, an electronic fuel injector model was built according to Payri et al. [37] and completely validated by the experimental data disclosed in that article. Then, this validated injector model was included in a DOE model, where a Uniform Latin Hypercube method was adopted. Then, the effects of these fuel properties on the injector dynamic response were compared and shown by RSM function charts from a statistical point of view, in which an SS-ANOVA method was adopted.

DOE is a systematic method for building a relationship between the input factors and output factors of a process. A great deal of information can be obtained through a reduced number of DOE simulations; therefore, it is effective to investigate the influences of individual variables on the response. In DOE, "factors" refer to design variables, and "level" refers to a specific value assigned to a factor. A DOE method creates a number of design points, which is a variation in the selected model's parameters [39].

The ULH is one of the most commonly used DOE methods. In it, the design space of each factor or design parameter is divided into n uniform levels. On each level of every factor, only one design point is placed. For each factor, $n!$ permutations of the n levels are possible. The design matrix of the ULH consists of one column for each factor, which is determined by a

randomly chosen permutation of the n levels. For a row of the design matrix, n^k combinations are possible and have an equal chance of occurring. As the matrix is generated randomly, a correlation between the columns may exist [40].

The RSM is frequently used as a tool for building an approximation model based on the data generated through DOE [41]. Several methods can be adopted to build this model, such as polynomials, SS-ANOVA, NN, k-nearest, etc. SS-ANOVA is a statistical modelling algorithm based on a function decomposition similar to the classical analysis of variance (ANOVA) decomposition and the associated notions of main effect and interaction. It belongs to the family of nonparametric or semi-parametric models and shows some peculiarities such as the interpretability of the results, which distinguishes from the classical set of standard parametric models (polynomial models, etc.). It is suitable for both univariate and multivariate modelling/regression problems [42]. The SS-ANOVA [43] was adopted here for data analysis.

2. The injector model and its validation

The injector model can be built either by a set of ordinary differential equations or some advanced tools, i.e., Hydsim and AMESim software. Here, the fuel injector model was built in AMEsim software, as shown in Fig. 1. The model consisted of three different parts: the injector holder, the electro-valve and the nozzle. Each of its internal elements were geometrically characterised by using a silicone moulding technique [44] together with Scanning Electron Microscopy (SEM) images. The silicone moulding technique has been proven to be an accurate and useful tool for obtaining the geometry of different components. In addition, the hydraulic characteristic of some most important orifices, i.e. the control oil inlet/outlet orifices, and the nozzle orifices, were tested in purpose-made test rigs [37, 38]. In this model, some assumptions were made: (1) all the variations are isothermal; and so, the fuel temperature and the fuel

properties were assumed to be constant along the injector and equal to those at the injector inlet [32]; (2) the pressure feeding the model is constant; therefore, it ignores the pressure fluctuations caused by the cyclical oil supply from the high-pressure pumps.

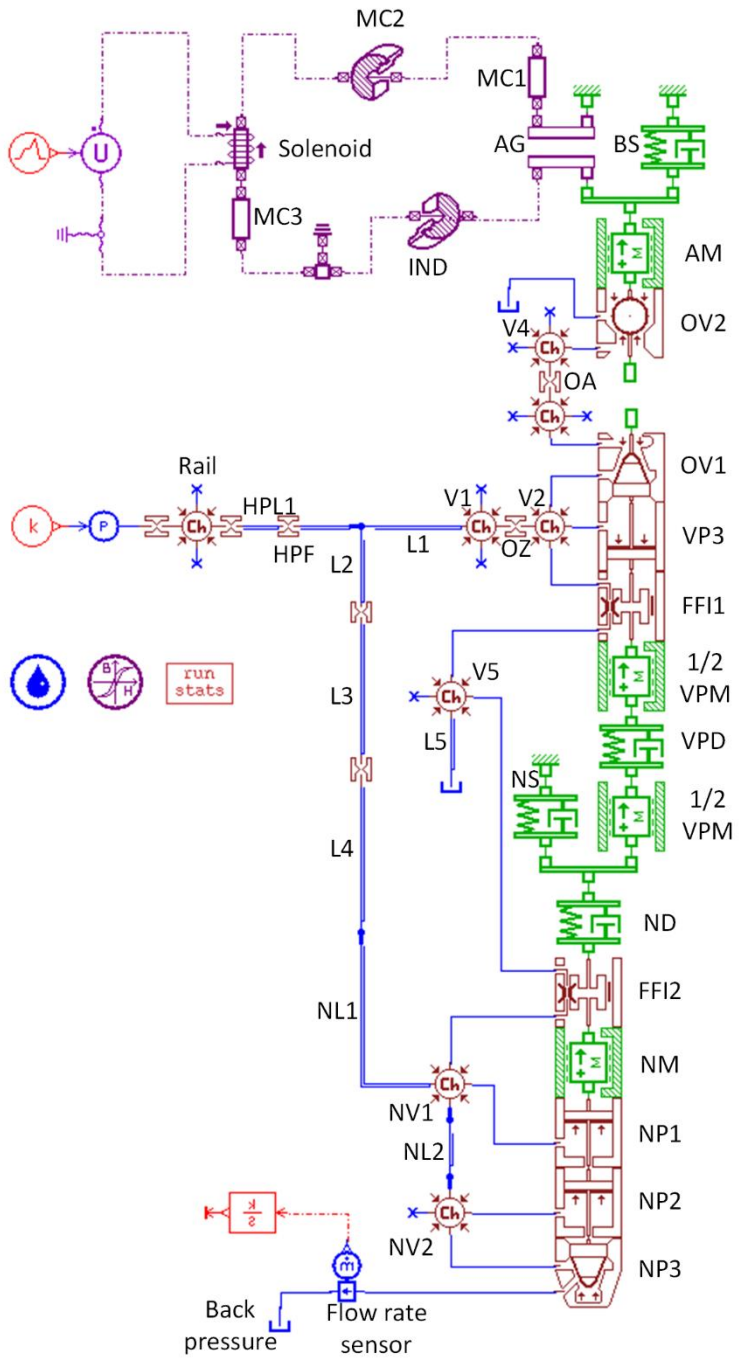

Fig. 1 One-dimensional fuel injector model

The model was validated by the experimental injection rate and injection quantities of 30 MPa, 80 MPa and 130 MPa rail pressures. Three different activation times, i.e., 0.5 ms, 1 ms and 2 ms, were applied. The comparisons of the injection rate and the injection quantity are shown in Fig. 2 and Fig. 3 respectively. Detailed values of the injection quantity are shown in Table 1. From Fig. 2, the simulation injection rates show an identical tendency at the end of needle valve closing are much lower than the experimental results. This can be attributed to the elastic differences in the material between an injector model and an authentic fuel injector. The authentic fuel injector has an elastic body. Thus, when the injector is deactivated, the needle valve moves back to its original place and hits on the seat. The needle valve bounces back several times before it closes completely, which results in a small fuel injection rate in the experimental results. In Fig. 3，it can be seen that there is a small difference between the simulation results and experimental results, which becomes larger with an increase in the rail pressure. This is because a high rail pressure leads to a larger flow speed. When the cross-section area of the nozzle orifice is the same, a larger flow speed results in a larger injection quantity. However, these tiny differences in the injection rate and injection quantity can hardly have an impact on the injector dynamic response (opening/closing delay and opening/closing time), which are mainly decided by the injection rate slopes. Fig. 2 indicates that the injection rate slopes in all the sub-figures present a highly accurate reproduction of the experimental injection rate. Therefore, the injector model is precise enough and can be used for further study. For the detailed parameters of the injector model and the experimental data, refer to Payri et al. [37].

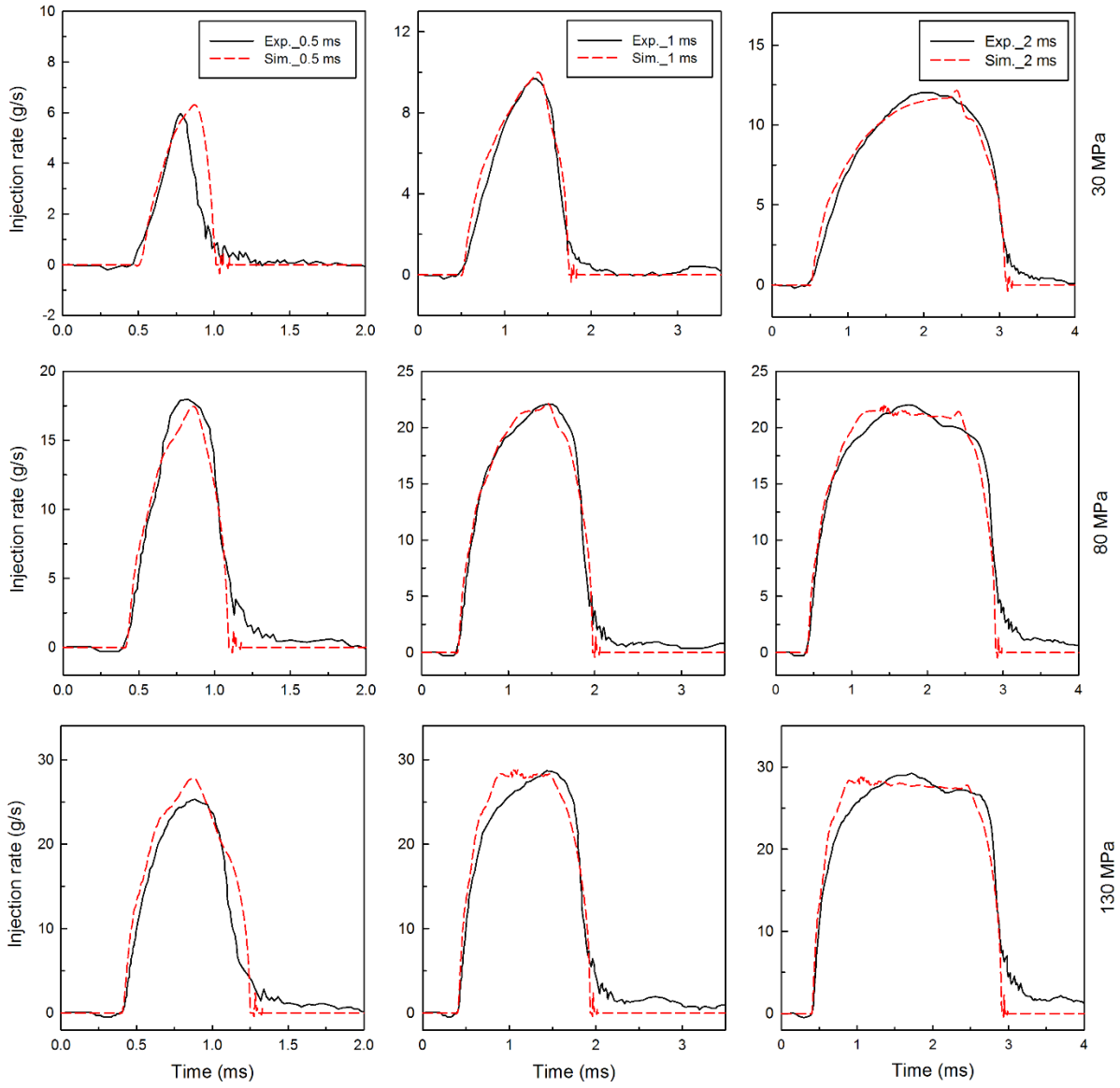

137

138 Fig. 2 Comparison of the injection rate under varies activation times and rail pressures

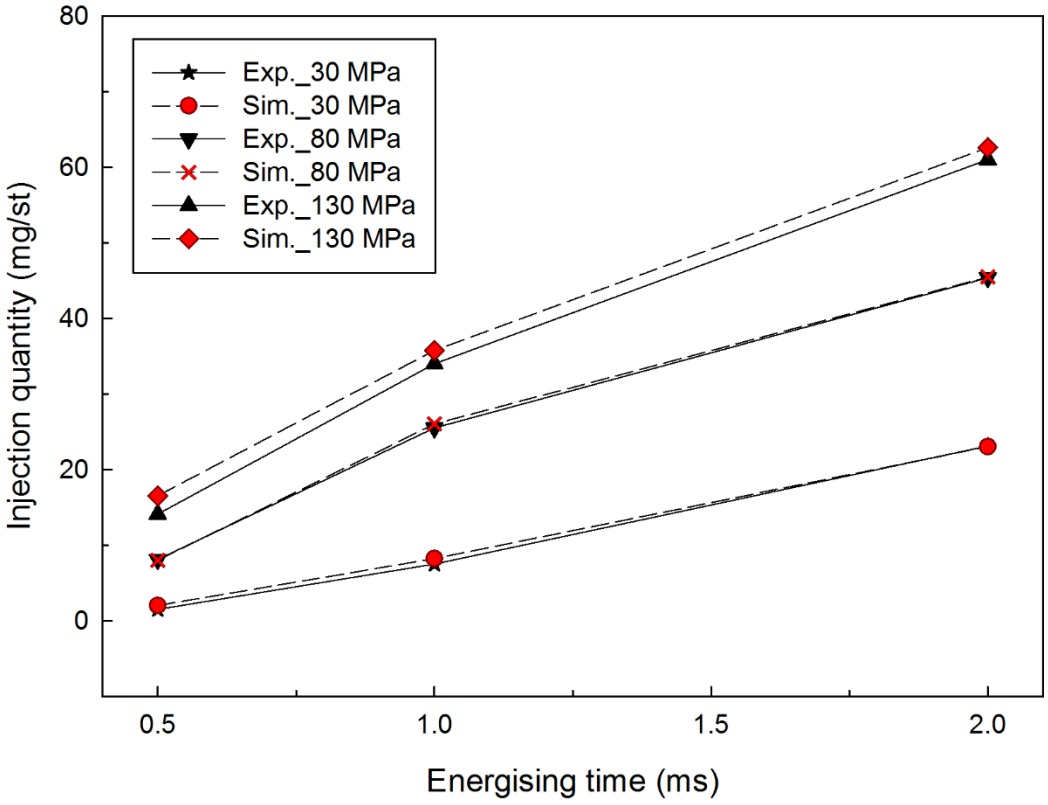

139

140 Fig. 3 Comparisons of the injection quantity under varies activation times and rail pressures

141 Table 1 Experimental and simulation injection quantity

Pressure	30 MPa		80 MPa		130 MPa	
Activate time	Exp., mg/st	Sim., mg/st	Exp., mg/st	Sim., mg/st	Exp., mg/st	Sim., mg/st
0.5 ms	1.5	2.0	8.1	8.0	14.1	16.5
1.0 ms	7.5	8.2	25.5	26.0	34.0	35.8
2.0 ms	23.1	23.0	45.4	45.5	61.0	62.6

3. Preparation

3.1. Definition of the injector dynamic response

The injector dynamic response refers to the needle valve opening/closing delay and needle valve opening/closing time, as shown in Fig. 4. The valve opening delay is defined as Δ T1, which is from the moment of t1 to the moment of T1; the valve opening time is defined as Δ T2, which is from the moment of T1 to the moment of T2; the valve closing delay is defined as Δ T3, which is from the moment of t3 to the moment of T3; and the valve closing time is defined as Δ T4, which is from the moment of T3 to the moment of T4.

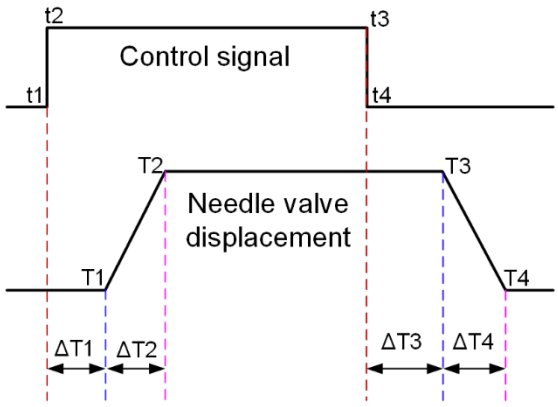

t1: the control signal initiates; t2: the control signal reaches its maximum amplitude; t3: the control signal begins to de-activate; t4: the control signal has fully disappeared; T1: the needle valve starts to open; T2: the needle valve has reached its maximum displacement; T3: the needle valve begins to close; T4: the needle valve has fully closed.

Fig. 4 Schematic diagram of the definition of the dynamic response

The injector dynamic response will simply be represented by a limited delay integrator transfer function:

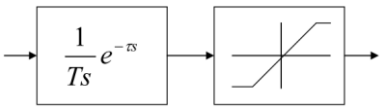

(1)

Where: T is the time constant; s is the field; τ is the delay.

3.2. DOE model

A DOE model was built within the modeFRONTIER software for investigating the effects of fuel properties on the dynamic response, as shown in Fig. 5. Firstly, a uniform Latin hypercube method was adopted in the DOE type for generating DOE designs, totally 1000 designs were generated. Then, the fuel injector model was included in the AMESim node. The control signal and the needle valve displacements generated by the fuel injector model were firstly written into a text file, and to do this, appropriate writing and reading rules needed to be specified. The text file is read by the MATLAB code, where the control signal opening/closing moments (t1, t2, t3 and t4) and the needle valve opening/closing moments (T1, T2, T3 and T4) are calculated [45]. Therefore, the valve opening/closing delay and the valve opening/closing time can be obtained. The simulation takes about 3 hours on an 8-core Intel i7-4790 CPU @ 3.60 GHz computer.

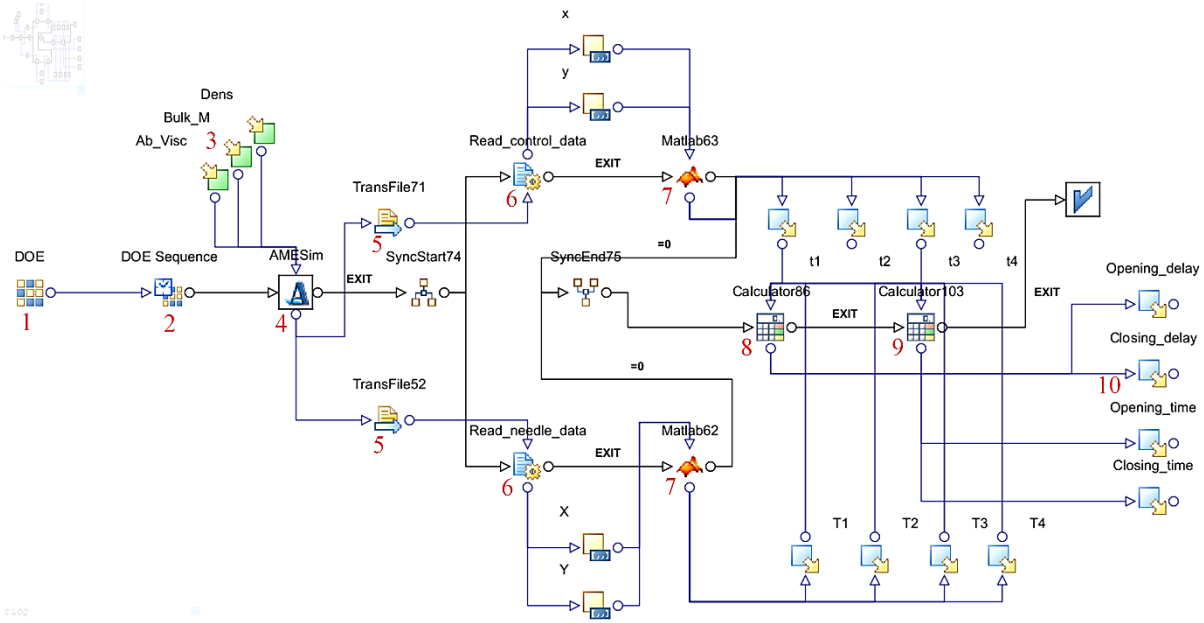

171

172 1: DOE designs generating; 2: DOE type selection; 3: Input parameters; 4: Fuel injector model; 5: Transfer the
173 control signal and needle valve displacement data synchronously; 6: Read the control signal and needle valve
174 displacement data from files respectively; 7: MATLAB codes; 8: Calculation of the valve opening/closing delay;
175 9: calculation of the valve opening/closing time; 10: Outputs.

176 Fig. 5 DOE model

177 **3.3. Boundaries and resolutions**

178 The boundaries of the three fuel properties derive from the Figure 2 of the reference [24]. In
179 that figure, the fuel properties of a stand winter diesel fuel are shown for a range of 0.1-300
180 MPa in pressure and 300-400 K in temperature. In the paper, the boundaries of a specific
181 pressure are set according to the minimum and the maximum values when the temperature
182 changes. Totally two pressures, including a low rail pressure (40 MPa) and a high rail pressure
183 (200 MPa) were applied. The details of the boundaries are shown in Table 2.

184 Table 2 Fuel properties and their boundaries for DOE

Input parameter	40 MPa	200 MPa	Step
Dens, kg/mm^3	764-848	860-920	2
Bulk_M, MPa	1150-1950	2750-3550	20
Ab_Visc, cP	0.1-5.9	2-46	0.2 for 40 MPa, 0.5 for 200 MPa

4. Results and discussion

4.1. Sensitivity analysis

The sensitivity of the three fuel properties on the dynamic response were compared at both the low rail pressure and at high rail pressure, as shown in the left part and right part of Fig. 6, respectively. They were examined and obtained by using a first order SS-ANOVA algorithm.

From Fig. 6 (a) and (b), it can be seen that the bulk modulus plays a dominant role in influencing the valve opening/closing delay at the low rail pressure. Interestingly, both the density and the bulk modulus have an dominant effect on the valve opening/closing time; the effects of the former are slightly larger than the latter, as shown in Fig. 6 (c) and (d). The bulk modulus affects the fluid's incompressibility. A large bulk modulus indicates that a larger pressure is needed to decrease the volume of a fluid. Therefore, a high incompressibility factor is provided by a fuel with a large bulk modulus. The fuel's incompressibility is one of the factors that affects the pressure wave's propagation speed and amplitude. Since the needle valve and the solenoid valve are hydraulic connected. The effects of bulk modulus are eventually reflected in the injector dynamic response. Density has an impact on the inertia resistance and on the pressure wave propagation speed. Therefore, the density also profoundly affects the dynamic response. The relationship of the bulk modulus and density with the speed of sound is shown in equation(2):

$$v = \sqrt{\frac{B}{\rho}} \tag{2}$$

Where, v is the speed of sound in the fluid; B is the bulk modulus of the fluid; and ρ is the density of the fluid.

The right part of Fig. 6 indicates that the effects of the absolute viscosity and the bulk modulus are influential on the dynamic response of the injector at the high pressure, and the former plays a dominant role in the valve opening/closing time. This is because viscosity drastically increases at high pressures. Viscosity is related to the friction force, which impedes the movements of the needle valve. Since the fuel oil in the control chamber flows in a laminar form. The pressure loss is proportional to the friction coefficient, fluid density and fluid velocity, as shown in equation (3) [30]:

$$\Delta P = C_f \frac{L}{D} \frac{\rho u^2}{2} \tag{3}$$

Where, C_f is the friction coefficient; ρ is the fluid density, kg/m^3; u is the fluid velocity, m/s; L is the pipe length, m; D is the pipe diameter, m.

The friction coefficient of a fluid flow in laminar conditions can be calculated as:

$$C_f = \frac{64}{R_e} = \frac{64\mu}{\rho u D} \tag{4}$$

Where, μ is the absolute viscosity, Pa·s; R_e is the Reynolds number [46, 30].

From (4), it can be seen that the friction coefficient is proportional to the absolute viscosity. Therefore, the absolute viscosity is also an influential factor and is significant to the injector dynamic response.

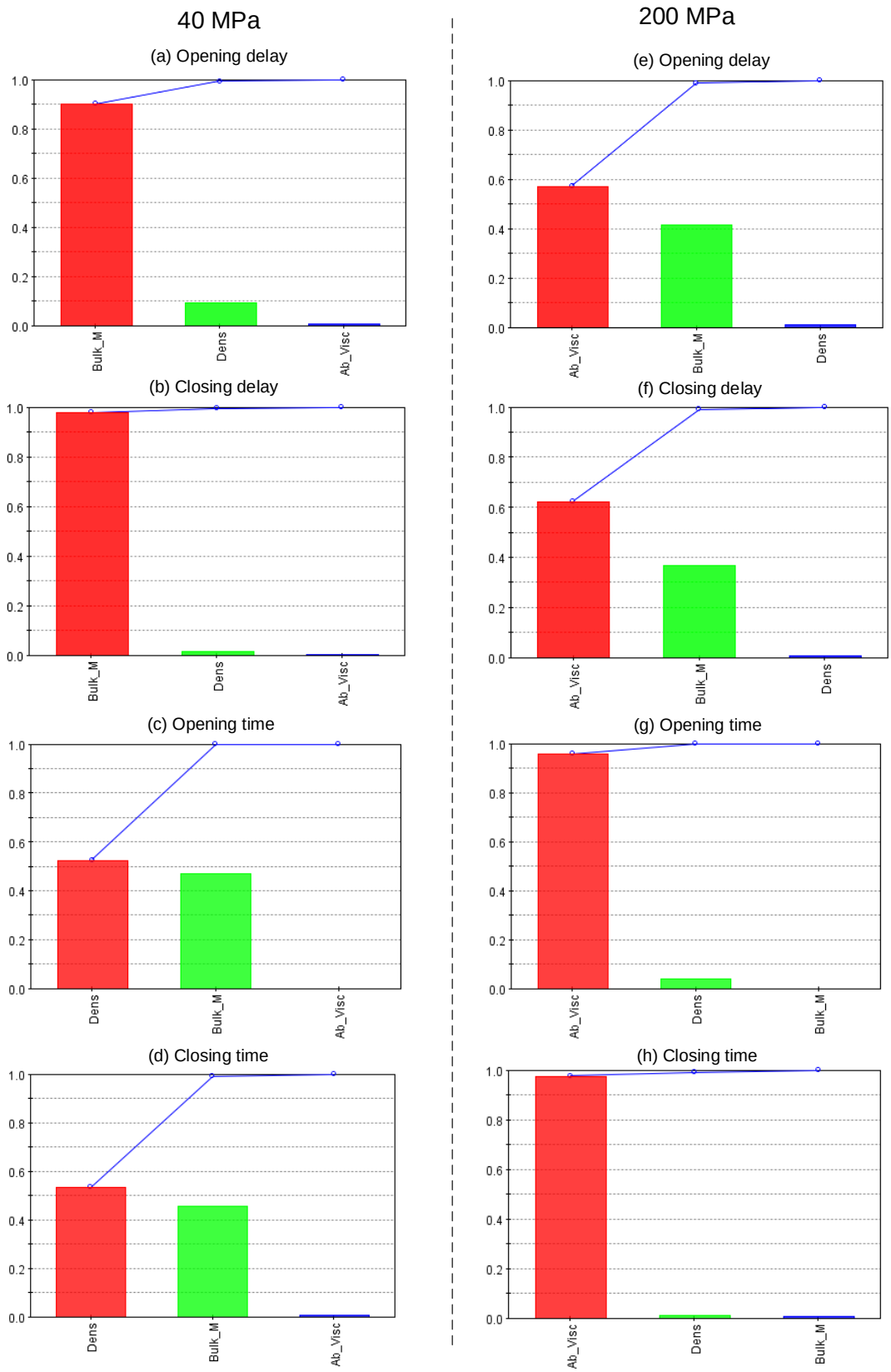

Fig. 6 Sensitivity of fuel properties on the injector dynamic response. (a) opening delay at 40 MPa rail pressure; (b) closing delay at 40 MPa rail pressure; (c) opening time at 40 MPa rail pressure; (d) closing time at 40 MPa

rail pressure; (e) opening delay at 200 MPa rail pressure; (f) closing delay at 200 MPa rail pressure; (g) opening time at 200 MPa rail pressure; (h) closing time at 200 MPa rail pressure.

The effects of the bulk modulus, density and absolute viscosity on the dynamic response are shown in Fig. 8, Fig. 14 and Fig. 19 respectively. They were generated by the RSM function, with only one factor changing at a time.

4.2. Effects of the bulk modulus

The trends of the effects of the bulk modulus are identical at both the low and the high rail pressures, as are the effects of the fuel density. Since the bulk modulus and the density were influential at the low pressure, only those effects are presented, as shown in Fig. 8, in which the effects are shown as red lines.

It is well known that the valve opening time and the valve closing time depend on the pressure difference between the control chamber and the accumulation chamber. Therefore, the pressures in the control chamber and the accumulation chamber are shown in Fig. 9, and the details of Section A and Section B are reported in Fig. 10 and Fig. 11, respectively. In these figures, only three different values of the bulk modulus were reported in order to get a clear view of the differences in the pressures. The pressures in the control chamber and the accumulation chamber were drawn in thick lines and in thin lines respectively. The same colour in a figure indicates the same value of factors. The above rules also apply to Fig. 14, Fig. 15, Fig. 16, Fig. 19, Fig. 20 and Fig. 21.

In order to obtain a better understanding of the pressure fluctuation in the control chamber. A theoretical pressure fluctuation prediction was given before the simulation pressure fluctuation

was investigated. This is presented along with the displacements of the solenoid valve and the needle valve opening/closing, as shown in Fig. 7. The pressure in the control chamber is identical to the rail pressure p_r before the solenoid valve is activated; when it is activated, it leads to a continual pressure drop in the control chamber. When the pressure decreases to the critical pressure p_{co}, it triggers the needle valve to open. During this process, the pressure in the control chamber increases slightly. However, the pressure drops again to a lower and steady pressure when the needle valve and the solenoid valve are both fully opened. When the solenoid valve is deactivated and fully closed, the pressure in the control chamber is regaining the rail pressure to push the needle valve to close. During this period of time, the pressure in the control chamber decreases slightly and then rockets up to the level of the rail pressure once the needle valve is completely closed.

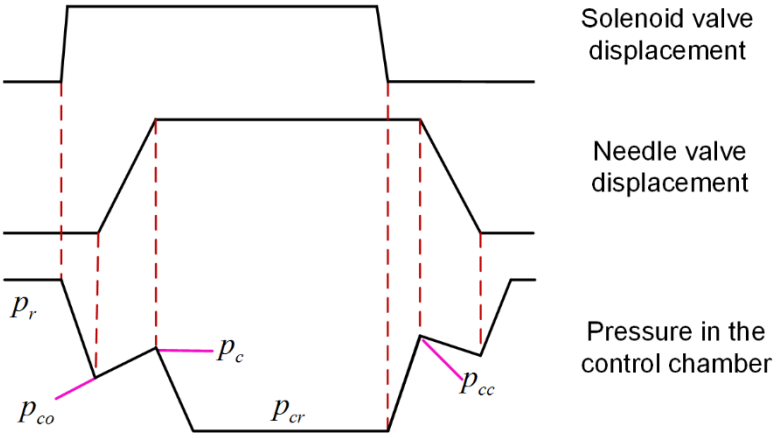

Fig. 7 Pressure change in the control chamber

From Fig. 8 (a) and (b), it can be seen that both the valve opening delay and the valve closing delay decrease with an increase in the bulk modulus. From equation(2), it can be deduced that the speed of sound through the fluid increases with an increase in the bulk modulus. A large bulk modulus indicates a fast pressure wave propagation. This leads to an advanced pressure

fluctuation. Therefore, the pressure in the control chamber drops faster when the solenoid valve is activated than in a fluid with a small bulk modulus, as shown in Fig. 10; the fast pressure wave propagation also results in a faster pressure rise when the solenoid is deactivated, as shown in Fig. 11. In these conditions, a small valve opening delay and valve closing delay were seen in the large bulk modulus case. In addition, Fig. 10 also indicates that the advanced pressure fluctuation leads to a lower critical opening pressure p_{co}, which would result in a larger pressure difference at the early stage of the needle valve opening. As is stated above, a large pressure difference is beneficial for a small valve opening delay; however, the large pressure difference changed to a small one at the later stage of the needle valve opening, as shown in the middle part of Fig. 9. A small pressure difference indicates a small force difference, which provides a small net force to push the needle valve upwards when the solenoid is activated; this leads to a slow needle movement, and thus a large valve opening time. In general, a large valve opening time is due to a large bulk modulus, as shown in Fig. 8 (c). However, the small pressure difference provides less resistance to the needle valve movements when the solenoid is deactivated. Thus, a small valve closing time is seen, as shown in Fig. 8 (d). The needle valve displacements under different bulk moduli are shown in Fig. 12. The needle valve opens earlier but reaches its maximum position later in cases with a larger bulk modulus, as opposed to those with a small bulk modulus. However, the needle valve closes and moves back to its original place in advance. The results shown in Fig. 12 agree with those shown in Fig. 7.

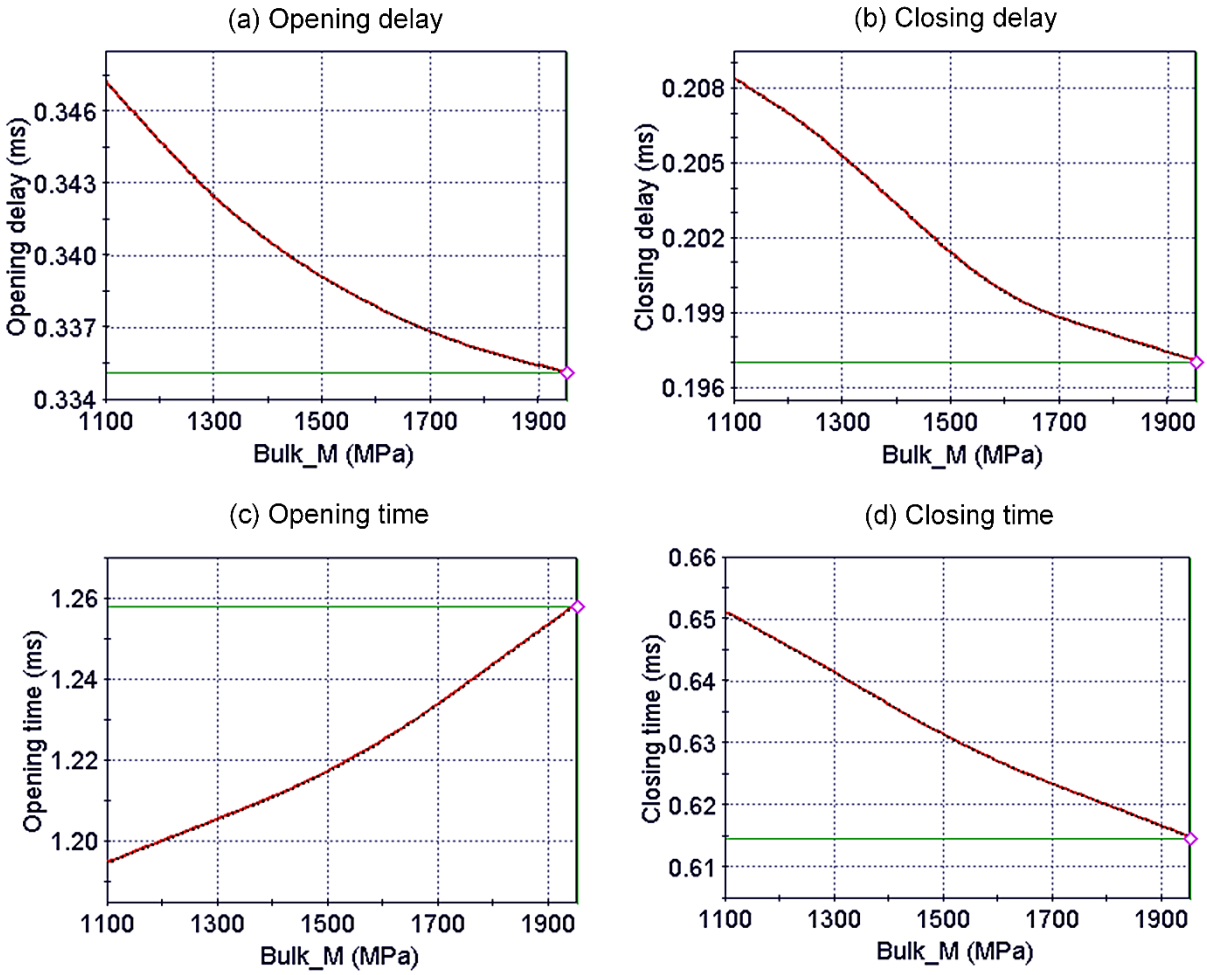

282

283 Fig. 8 Effects of the bulk modulus on the dynamic response at 40 MPa rail pressure

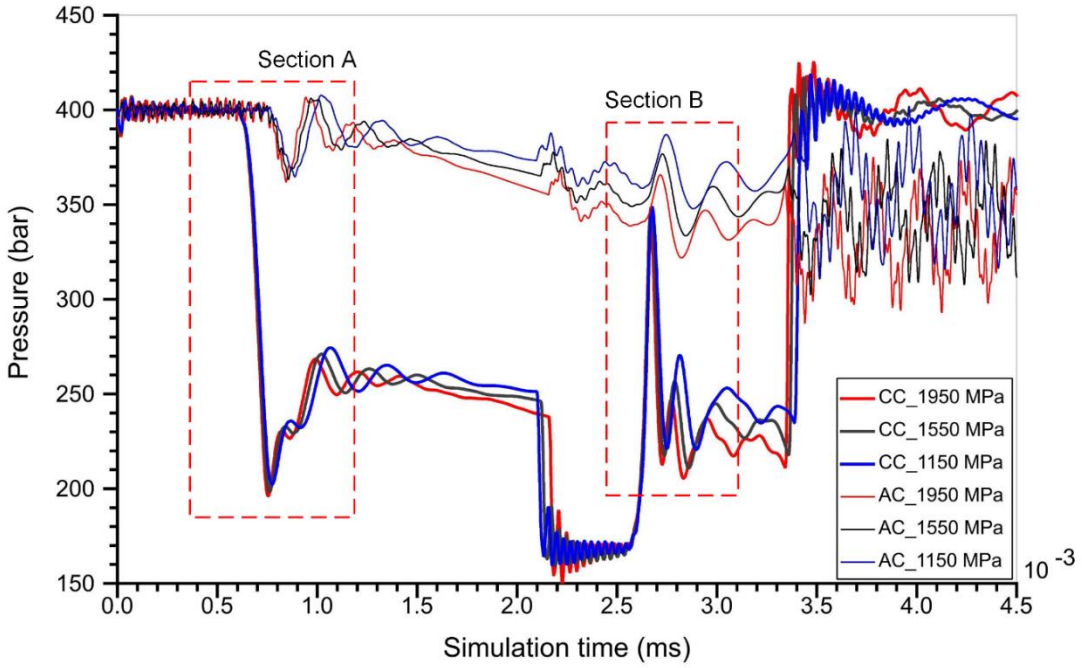

284

285 Fig. 9 Pressure in the control chamber and in the accumulation chamber at the low rail pressure

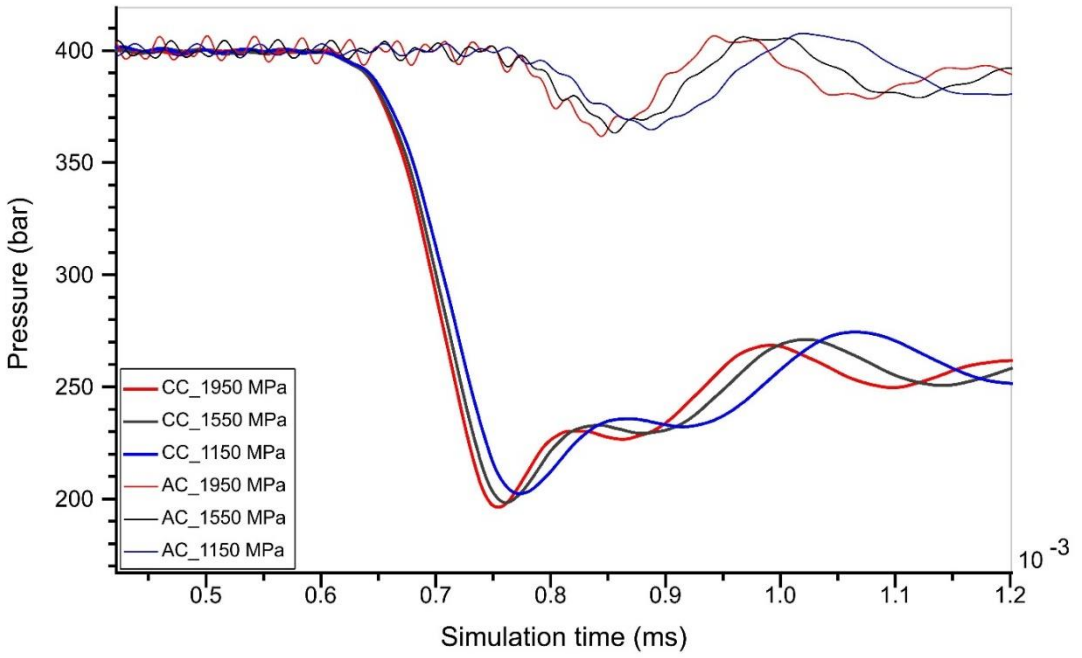

286

287 Fig. 10 Details of Section A in Fig. 9

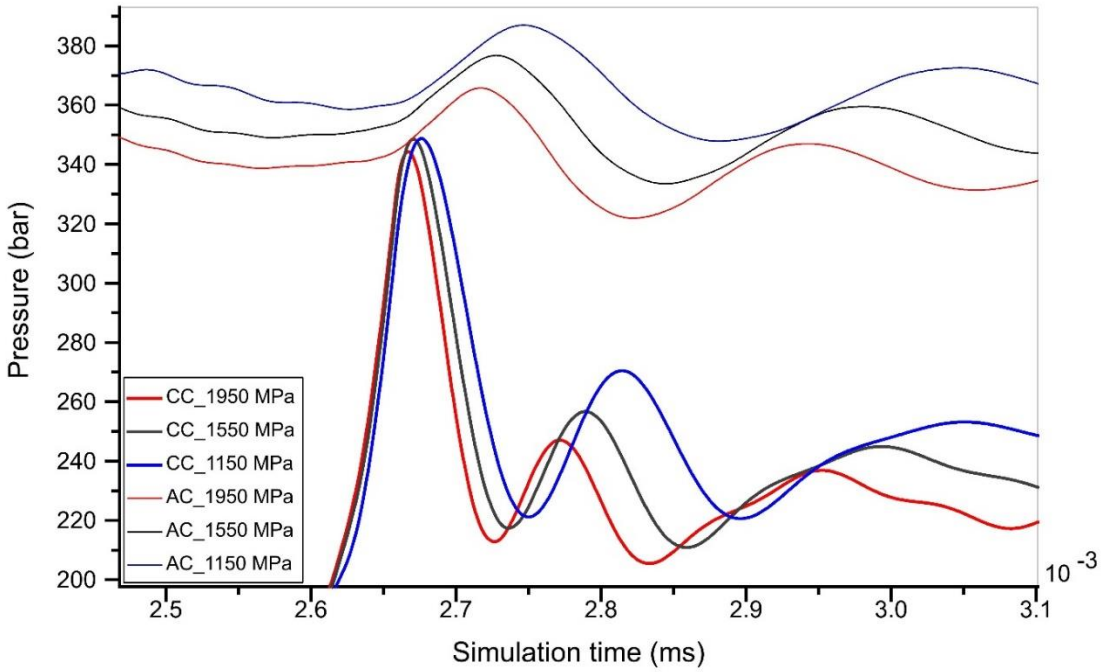

288

289 Fig. 11 Details of Section B of Fig. 9

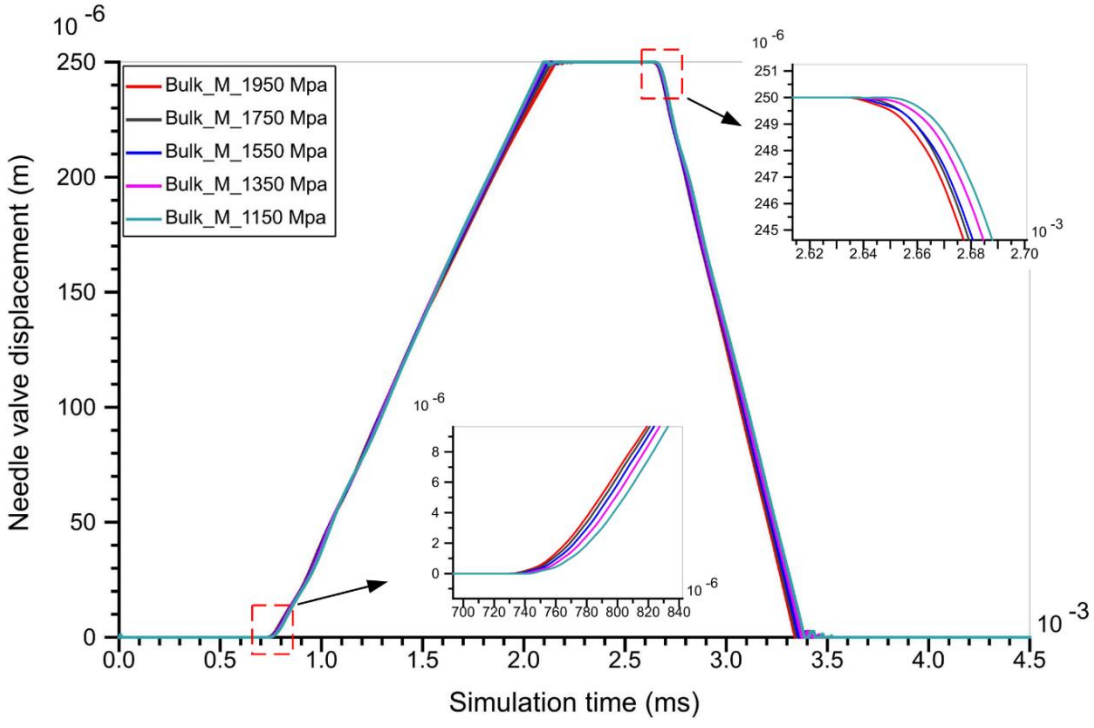

290

291 Fig. 12 Needle valve displacements under different bulk modulus conditions

4.3. Effects of the fuel density

A high fuel density contributes to increasing the valve opening/closing delay and the valve opening/closing time, as shown in Fig. 13. A high density indicates a large inertia; therefore, it retards the pressure wave propagation (as shown in Fig. 15 and Fig. 16) and results in a large resistance to the movements of the needle valve at both the valve opening and valve closing stages (as shown in Fig. 17). The retarded pressure wave propagation leads to large hydraulic delays (valve opening/closing delay), and the large inertia resistance is the main reason for the increased valve opening/closing time in high-density conditions.

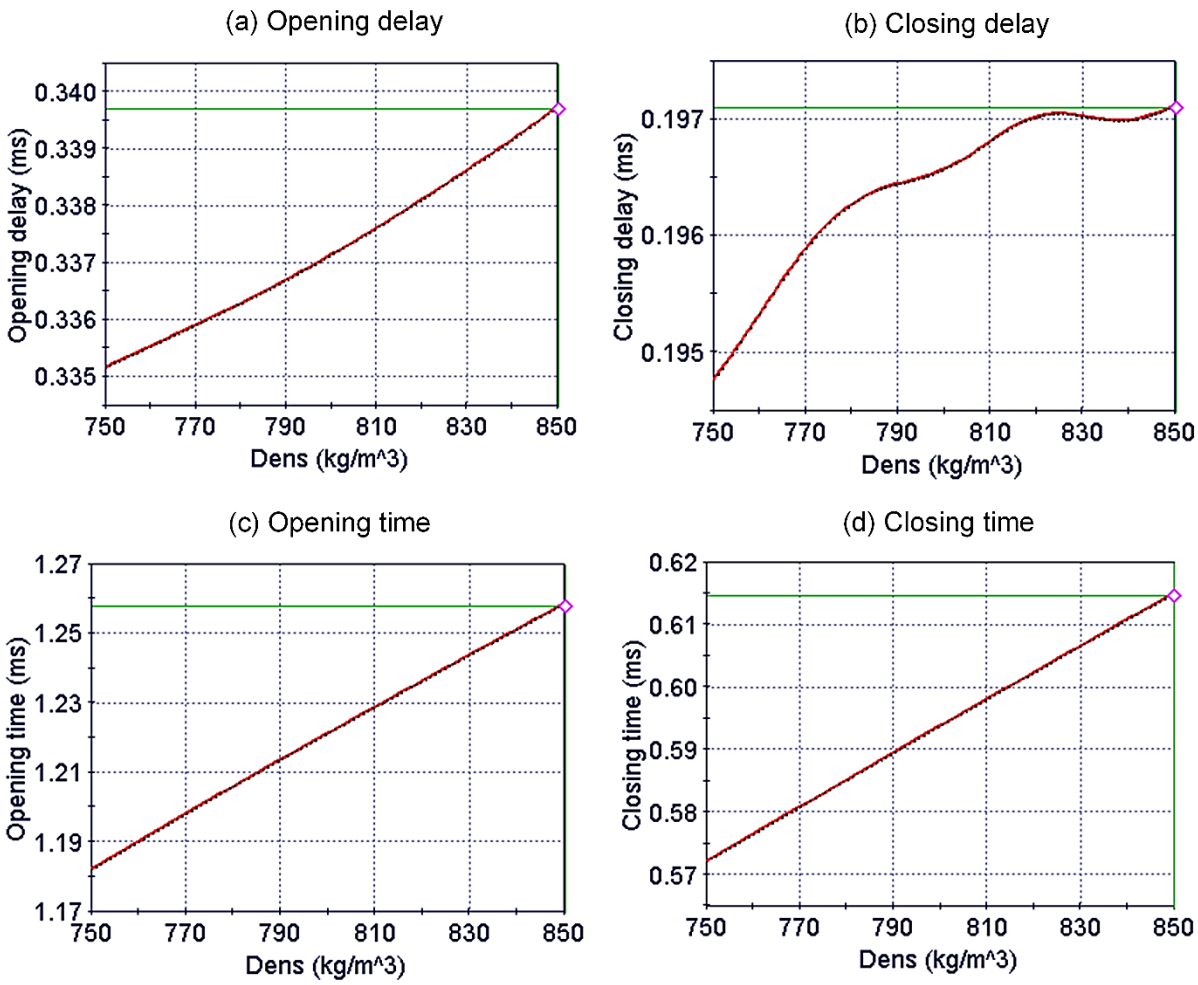

Fig. 13 Effects of the density on the dynamic response at 40 MPa rail pressure

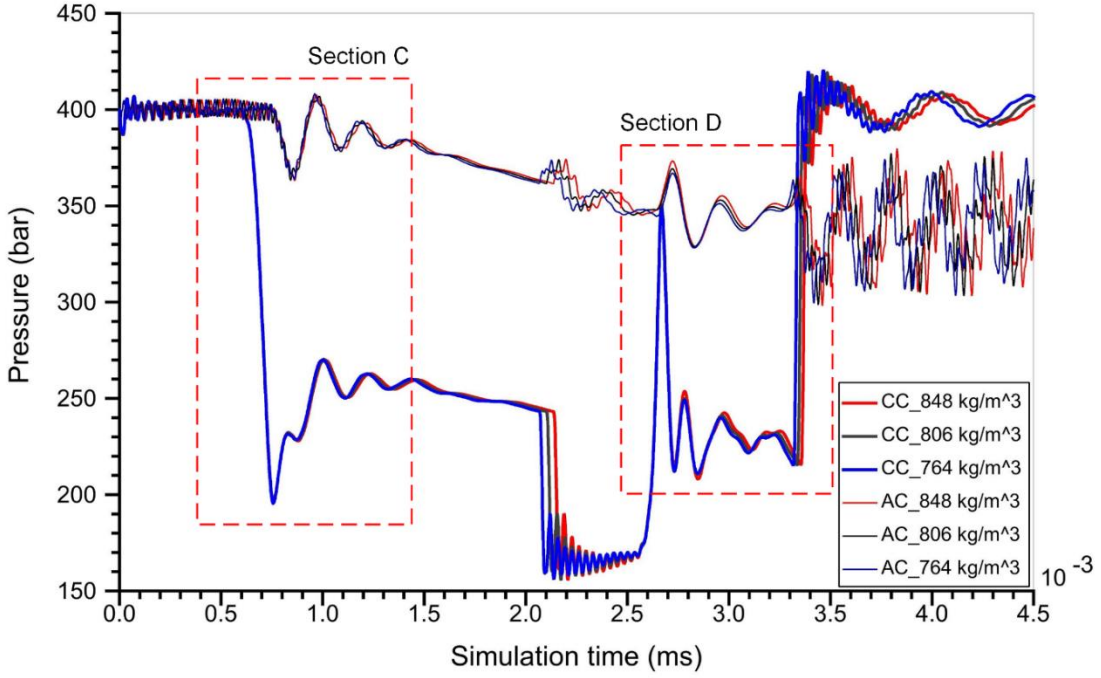

302

303 Fig. 14 Pressure in the control chamber and in the accumulation chamber at the low rail pressure

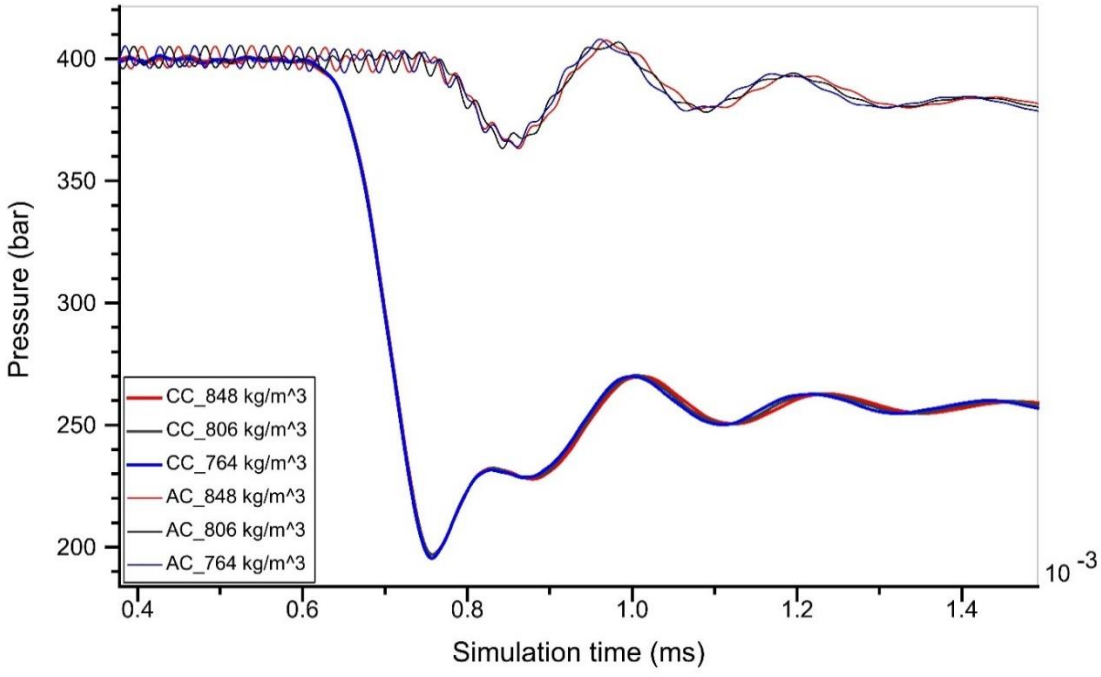

304

305 Fig. 15 Details of Section C in Fig. 14

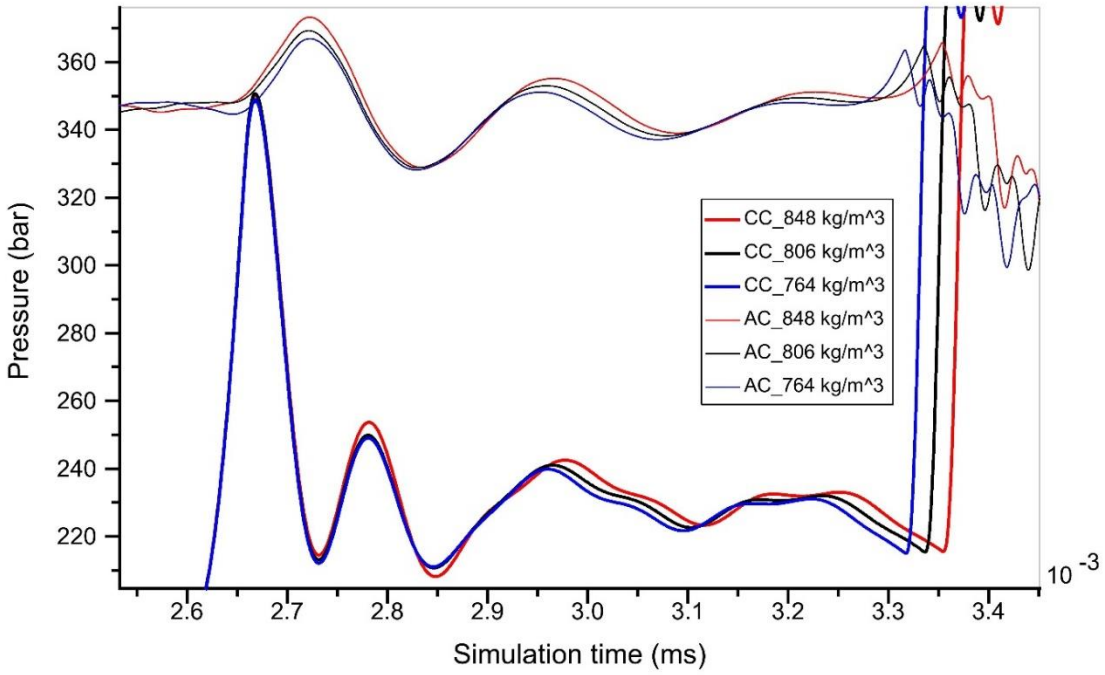

306

307 Fig. 16 Details of Section D in Fig. 14

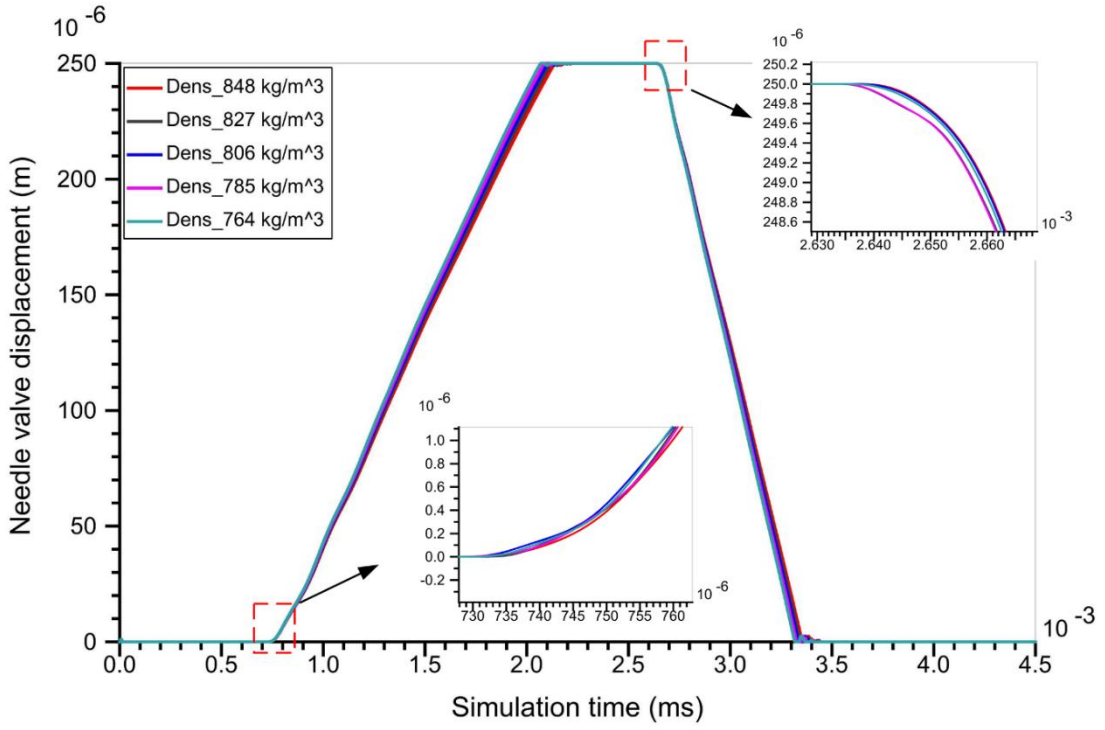

308

309 Fig. 17 Needle valve displacements in different fuel density conditions

4.4. Effects of the viscosity

At the high rail pressure, the viscosity varies over a much bigger range with a change in temperature, than at the low rail pressure. A high viscosity suppresses the amplitude of the pressure wave and leads to a quick dampening rate [30]. In addition, from equations (3) and (4), it can be inferred that a high viscosity results in a large pressure loss in the control chamber.

A quicker pressure wave dampening rate means the pressure in the control chamber reaches the critical valve opening pressure in a shorter time when the solenoid is activated, as shown in Fig. 20. Therefore, a high fuel viscosity results in a small valve opening delay, as shown in Fig. 18 (a). A large pressure loss in the control chamber leads to a slightly lower steady pressure when the needle valve is fully opened, as shown in Fig. 19. This lower steady pressure also means that a larger pressure difference exists between the control chamber and the accumulation chamber. As stated previously, the pressure difference plays a dominant role in the valve opening and valve closing times. Although the friction force increases with the increase in viscosity, the friction force is still not comparable to the force generated by the pressure difference, as shown in Fig. 22. Therefore, a high viscosity generates a large pressure difference, which accelerates the needle movement to achieve a short valve opening time at the needle valve opening stage, and slows down the needle action when it is returning to its seat, which results in a large valve closing time, as shown in Fig. 18 (c) and (d). Additionally, the slightly lower steady pressure indicates that it takes a longer time to restore the critical valve closing pressure. Therefore, a larger valve closing delay is seen, as shown in Fig. 18 (b). Detailed needle movements are shown in Fig. 23.

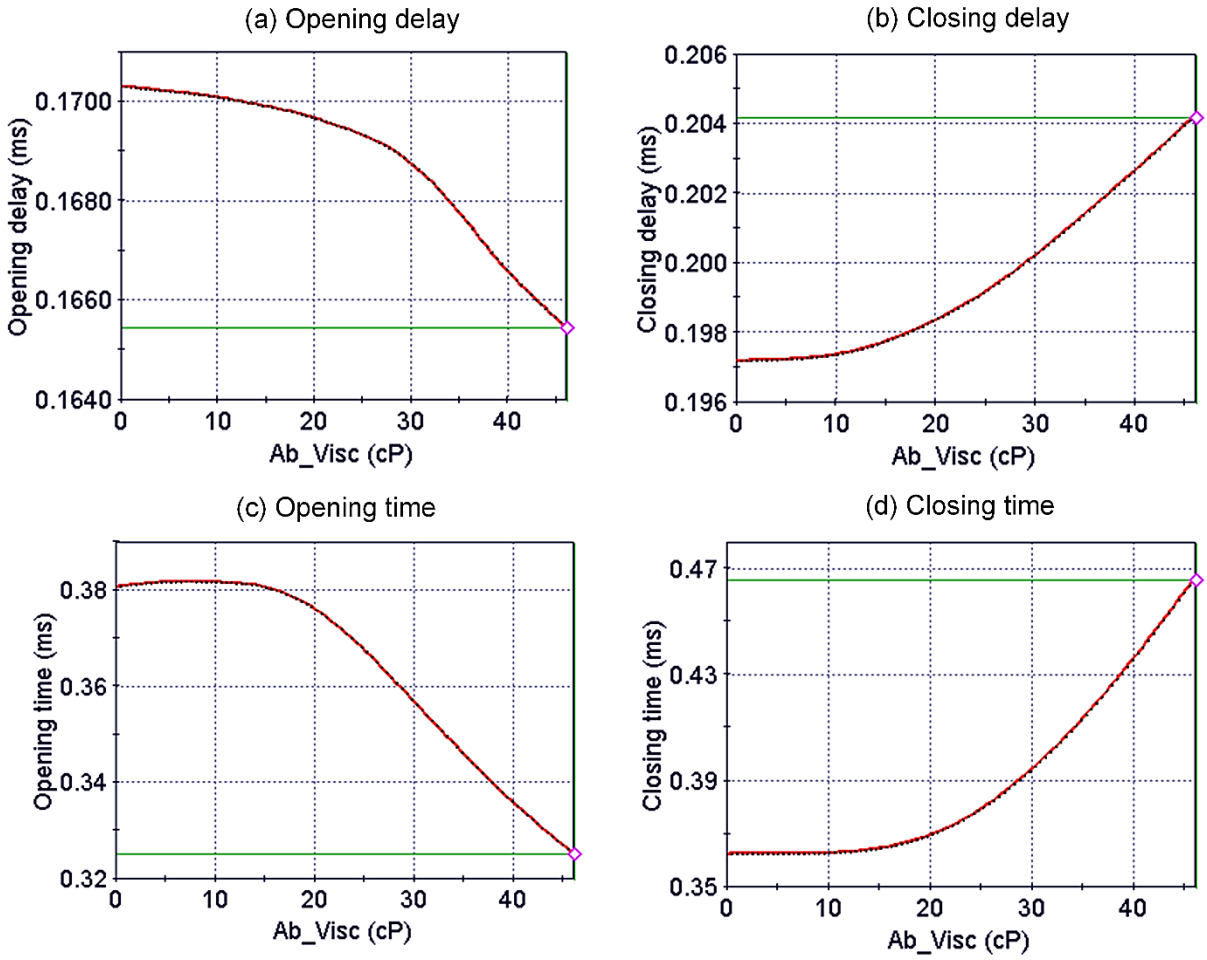

331

332 Fig. 18 Effects of the absolute viscosity on the dynamic response at 200 MPa rail pressure

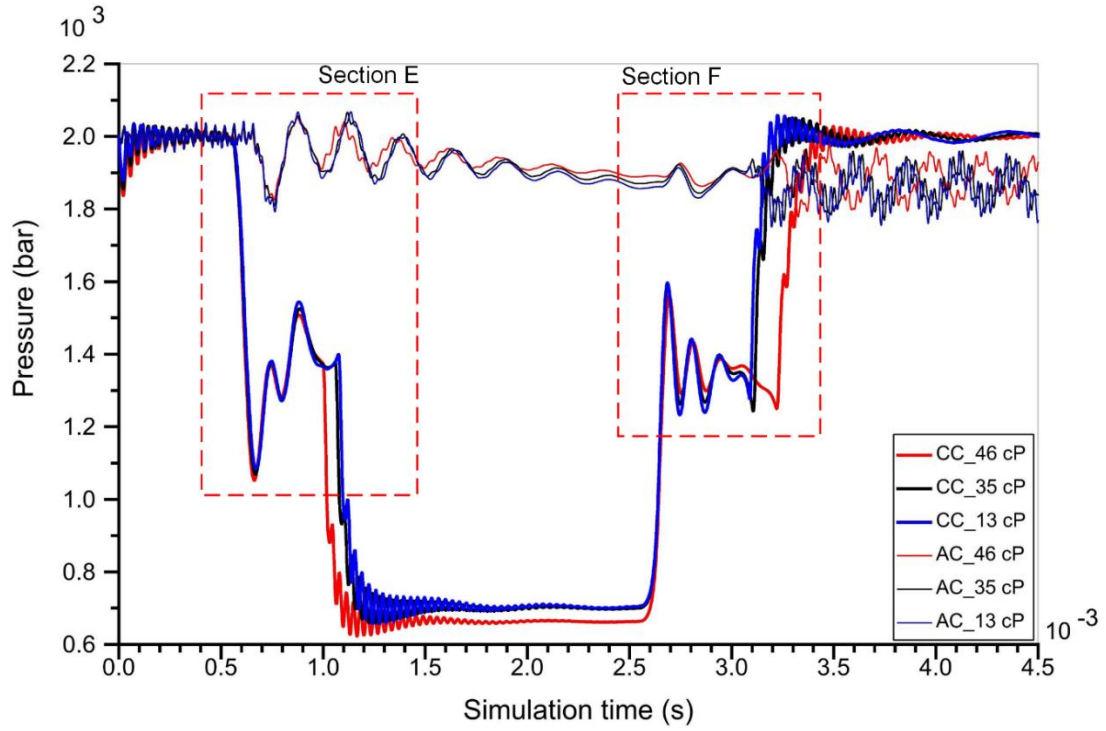

333

334 Fig. 19 Pressure in the control chamber and in the accumulation chamber at the high rail pressure

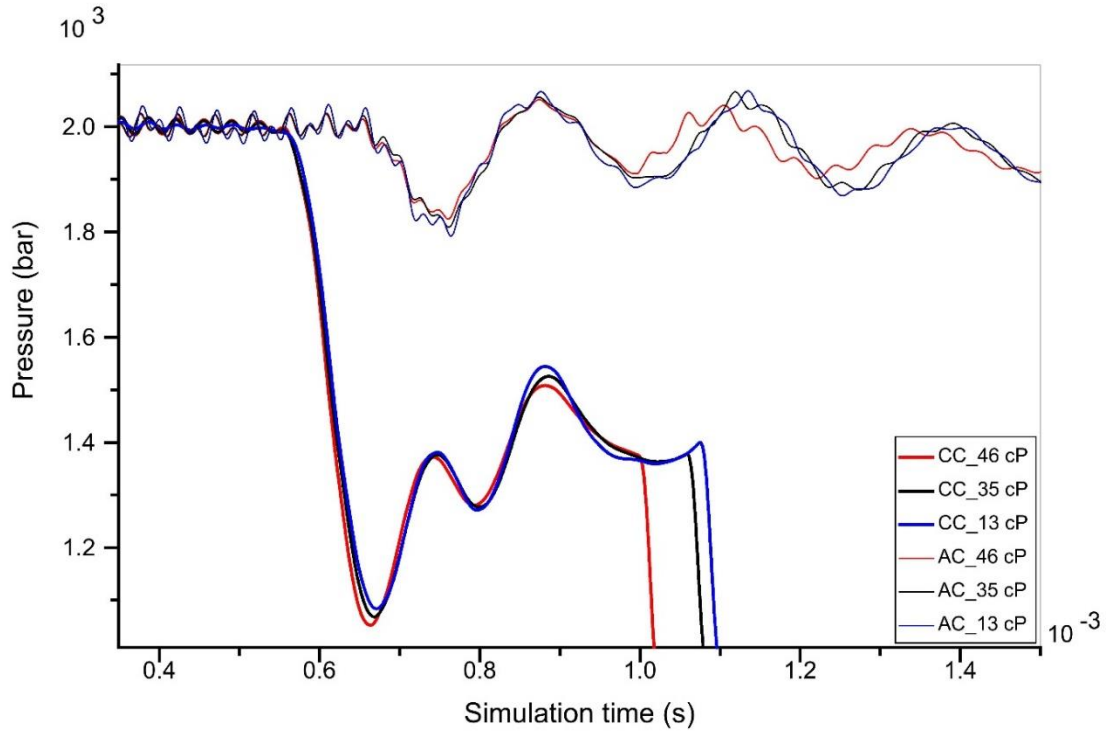

335

336 Fig. 20 Details of Section E in Fig. 19

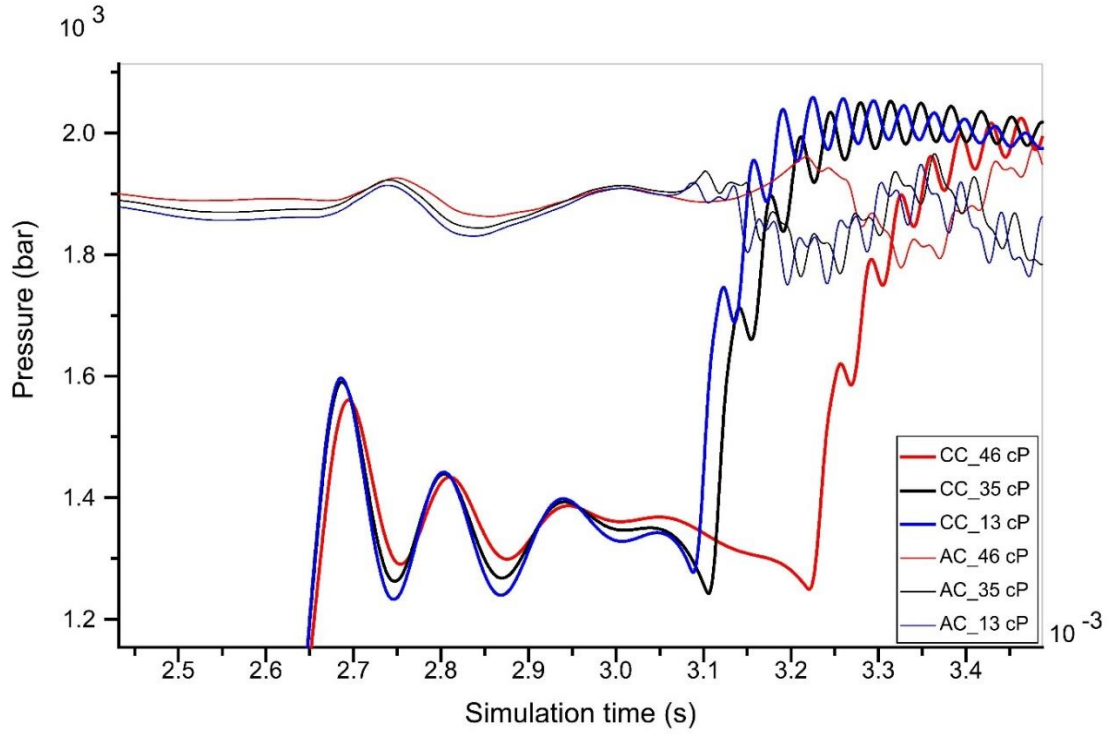

337

338 Fig. 21 Details of Section F in Fig. 19

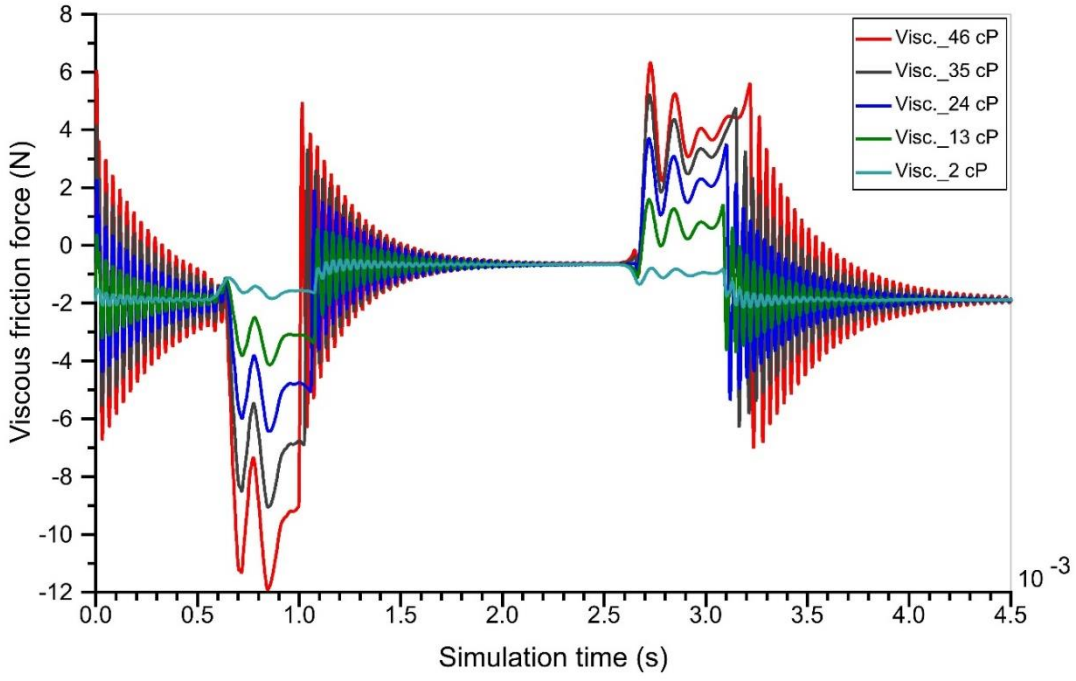

339

340 Fig. 22 Friction forces under different absolute viscosities

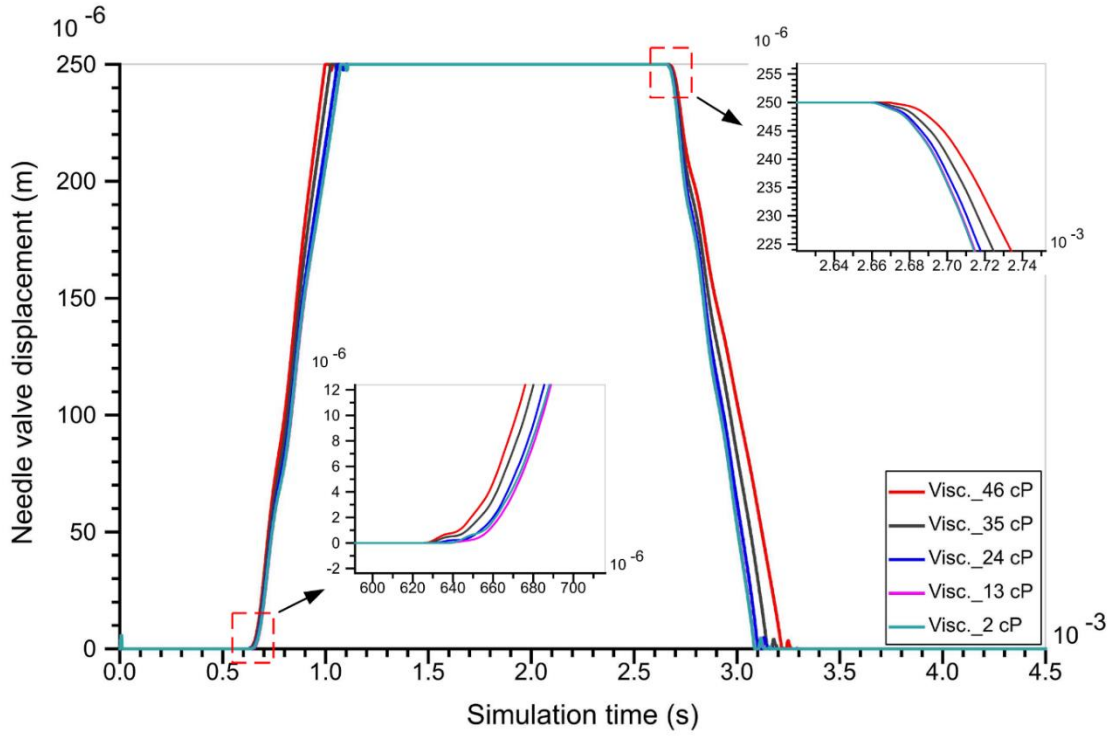

Fig. 23 Needle valve displacements under different absolute viscosity conditions

5. Conclusions

The effects of fuel properties (bulk modulus, density and absolute viscosity) on the injector valve opening/closing delay and valve opening/closing time were investigated individually. A fuel injector model was built and validated by injection rate and injection mass at three different rail pressures. Then, a DOE model was built in modeFRONTIER software to study the effects of the fuel properties on the injector dynamic response from a statistical point of view. The effects of these properties were compared using an SS-ANOVA at both the low and high rail pressures. And then reported by RSM function charts based on the DOE data. In addition, the details of the pressure differences and needle valve movements were also presented. The main conclusions are as follows:

(1) The bulk modulus plays a dominant role in influencing the valve opening/closing delay at the low rail pressure.

(2) At the high pressure, however, the effects of the absolute viscosity are dominant, while the effects of the bulk modulus and the density are negligible.

(3) Both the valve opening delay and the valve closing delay decrease with an increase in the bulk modulus. A large valve opening time and a small valve closing time are the result of a large bulk modulus.

(4) A high fuel density results in an increase in the valve opening/closing delay and the valve opening/closing time, and vice versa.

(5) A high fuel viscosity results in a small valve opening delay and a large valve closing delay. In addition, it generates a large pressure difference, which accelerates the needle movement to achieve a short valve opening time, and slows down the needle valve movement when it is returning to its seat, to get a large valve closing time.

Acknowledgements

The authors are grateful to the Department of Naval Architecture, Ocean and Marine Engineering of the University of Strathclyde for its calculation support during the project.

Funding: This work was supported by the project ‘Engineering Development of a Medium-Speed Dual Fuel Engine (Ministry of Industry and Information Technology NO. (2013) 412,

371 2)' from China and the project 'An Investigation into the Characteristics of High-pressure
372 Common Rail Injection System' from Lloyds Register of Shipping in the UK.

373 ## References

[1] Benajes J, Pastor JV, Payri R, Plazas AH. Analysis of the influence of diesel nozzle geometry in the injection rate characteristics. J Fluids Eng. 2004; 126: 63-71.

[2] Han JS, Lu PH, Xie XB, Lai MC, Henein NA. Investigation of diesel spray primary breakup and development for different nozzle geometries. SAE Paper 2002; 2002-01-2775.

[3] Payri R, Garcia JM, Salvador FJ, Gimeno J. Using spray momentum flux measurements to understand the influence of diesel nozzle geometry on spray characteristics. Fuel 2005; 84: 551-561.

[4] Lahane S, Subramanian KA. Impact of nozzle holes configuration on fuel spray, wall impingement and NOx emission of a diesel engine for biodiesel-diesel blend (B20). Applied Thermal Engineering 2014; 64: 307-314.

[5] Salvador FJ, Martínez-López J, Caballer M, De Alfonso C. Study of the influence of the needle lift on the internal flow and cavitation phenomenon in diesel injector nozzles by CFD using RANS methods. Energy Conversion and Management 2013; 66: 246-256.

[6] Moon S, Gao Y, Park S, Wang J, Kurimoto N, Nishijima Y. Effect of the number and position of nozzle holes on in- and near-nozzle dynamic characteristics of diesel injection. Fuel 2015; 150: 112-122.

[7] He Z, Zhong W, Wang Q, Jiang Z, Fu Y. An investigation of transient nature of the cavitating flow in injector nozzles. Applied Thermal Engineering 2013; 54: 56-64.

[8] Payri F, Payri R, Salvador FJ, Martínez-López J. A contribution to the understanding of cavitation effects in Diesel injector nozzles through a combined experimental and computational investigation. Computers & Fluids 2012; 58: 88-101.

[9] Qiu T, Song X, Lei Y, Liu X, An X, Lai M. Influence of inlet pressure on cavitation flow in diesel nozzle. Applied Thermal Engineering 2016; 109: 364-372.

[10] He Z, Zhong W, Wang Q, Jiang Z, Fu Y. An investigation of transient nature of the cavitating flow in injector Nozzles. Applied Thermal Engineering 2013; 54: 46-64.

[11] Molina S, Salvador FJ, Carreres M, Jaramillo. A computational investigation on the influence of the use of elliptical orifices on the inner nozzle flow and cavitation development in diesel injector nozzles. Energy Conversion and Management 2014; 79: 114-127.

[12] Payri R, Salvador SJ. Gimeno J, Zapata LD. Diesel nozzle geometry influence on spray liquid-phase fuel penetration in evaporative conditions. Fuel 2008; 87: 1165-1176.

[13] Payri R, Salvador SJ. Gimeno J, Morena J. Effects of nozzle geometry on direct injection diesel engine combustion process. Applied Thermal Engineering 2009; 29: 2051-2060.

[14] Wang B, Badawy T, Jiang Y, Xu H, Ghafourian A, Zhang X. Investigation of deposit effect on multi-hole injector spray characteristics and air/fuel mixing process. Fuel 2017; 191: 10-24.

[15] Payri R, Gimeno J, Bardi M, Plazas AH. Study liquid length penetration results obtained with a direct acting piezo electric injector. Applied Energy 2013; 106: 152-162.

[16] Payri R, Gimeno J, Viera JP, Plazas AH. Needle lift profile influence on the vapor phase penetration for a prototype diesel direct acting piezoelectric injector. Fuel 2013; 113: 257-265.

[17] Payri R, García-Oliver JM, Xuan T, Bardi M. A study on diesel spray tip penetration and radial expansion under reacting conditions. Applied Thermal Engineering 2015; 90: 619-629.

[18] Payri R, Viera JP, Pei YJ, Som S. Experimental and numerical study of lift-off length and ignition delay of a two-component diesel surrogate. Fuel 2015; 158: 957-967.

[19] Payri R, Salvador FJ, Manin J, Viera A. Diesel ignition delay and lift-off length through different methodologies using a multi-hole injector. Applied Energy 2016; 162: 541-550.

[20] Crookes RJ, Bob-Manuel KDH. RME or DME: A preferred alternative fuel option for future diesel engine operation. Energy Conversion and Management 2007, 48(11): 2971-2977.

[21] Cheng Q, Xu M, Zhang Z, Xie N. Investigation on the spray characteristics of standard gasoline, n-pentane, iso-octane and ethnaol with a novel heated tip SIDI injector. Applied Thermal Engineering 2017, 110: 539-552.

[22] Dernotte J, Hespel C, Houillé S, Foucher F, Rousselle CM. Influence of fuel properties on the diesel injection process in nonvaporizing conditions. Atomization Sprays 2012; 22(6): 461-492.

[23] Payri R, Salvador FJ, Gimeno J, Bracho G. Effect of fuel properties on diesel spray development in extreme cold conditions. Proc Inst Mech Eng, Part D: J Automobile Eng 2008; 222: 1743-1753.

[24] Salvador FJ, De la Morena J, Martínez-López J, Jaramillo D. Assessment of compressibility effects on internal nozzle flow in diesel injectors at very high injection pressures. Energy Conversion and Management 2017, 132: 221-230.

[25] Desantes JM, Salvador FJ, Carreres M, Jaramillo D. Experimental characterization of the thermodynamic properties of diesel fuels over a wide range of pressures and temperatures. SAE Int J Fuels Lubricants 2015; 8(1): 190-199.

[26] Salvador FJ, Gimeno J, De la Morena J, Carreres M. Using one-dimensional modeling to analyze the influence of the use of biodiesels on the dynamic behavior of solenoid-operated injectors in common rail systems: Results of the simulations and discussion. Energy Conversion and Management 2012; 54: 122-132.

[27] Han D, Duan Y, Wang C, Lin H, Huang Z. Experimental study on injection characteristics of fatty acid esters on a diesel engine common rail system. Fuel 2014; 123: 19-25.

[28] Salvador FJ, Gimeno J, Carreres M, Crialesi-Esposito M. Fuel temperature influence on the performance of a last generation common-rail diesel ballistic injector. Part I: Experimental

mass flow rate measurements and discussion. Energy Conversion and Management 2016; 114: 364-375.

[29] Payri R, Salvador FJ, Carreres M, De la Morena J. Fuel temperature influence on the performance of a last generation common-rail diesel ballistic injector. Part II: 1D model development, validation and analysis. Energy Conversion and Management 2016; 114: 376-391.

[30] Boudy F, Seers P. Impact of physical properties of biodiesel on the injection process in a common-rail direct injection system. Energy Conversion and Management 2009; 50: 2905-2912.

[31] Han D, Li K, Duan Y, Lin H, Huang Z. Numerical study on fuel physical effects on the split injection processeson a common rail injection system. Energy Conversion and Management 2017; 134: 47-58.

[32] Payri R, Salvador FJ, Carreres M, DelaMorena J. Fuel temperature influence on the performance of a last generation common-rail diesel ballistic injector. Part II: 1D model development, validation and analysis. Energy Conversion and Management 2016; 114: 376-391.

[33] Ando R, Koizumi M, Ishikawa T. Development of a simulation method for dynamic characteristics of fuel injector. IEEE TRANSACTIONS ON MAGNETICS 2001; 37 (5): 3715:3718.

[34] Seykens XLJ, Somers LMT, Baert RSG. Detailed modelling of common rail fuel injection process. J Middle Eur Construct Des Cars (MECCA) 2005; 3: 30-39.

[35] Rahim R, Mamat R, Taib MY, Abdullah AA. Influence of fuel temperature on diesel engine performance operating with biodiesel blend. J Mech Eng Sci. 2012; 2: 226-236.

[36] Bianchi GM, Falfari S, Pelloni P, Kong SC, Reitz RD. Numerical analysis of high-pressure fast-response common rail injector dynamics. SAE TECHNICAL PAPER SERIES 2002; 2002-01-0213.

[37] Payri R, Salvador FJ, Martí-Aldaraví P, Martínez-López J. Using one-dimensional modelling to analyse the influence of the use of biodiesels on the dynamic behaviour of solenoid-operated injectors in common rail systems: Detailed injection system model. Energy Conversion and Management 2012, 54: 90-99.

[38] Salvador FJ, Plazas AH, Gimeno J, Carreres M. Complete modelling of a piezo actuator last-generation injector for diesel injection systems. International J of Engine Research 2014; 15 (1): 3-19.

[39] Taghavifar H, Jafarmadar S, Taghavifar H, Navid A. Application of DoE evaluation to introduce the optimum injection strategy-chamber geometry of diesel engine using surrogate epsilon-SVR. Applied Thermal Engineering 2016, 106: 56-66.

[40] Cioppa TM, Lucas TW. Efficient Nearly Orthogonal and Space-Filling Latin Hypercubes. Technometrics 2007; 49(1): 45-55.

[41] Box GEP and Wilson KB. On the experimental attainment of optimum conditions (with discussion). Journal of the Royal Statistical Society Series B 1951; 13(1): 1-45.

[42] Rigoni E, Ricco L. Smoothing spline ANOVA for variable screening. ESTECO Technical Report 2011-007.

[43] Ali OM, Mamat R, Najafi G, Yusaf T, Ardebili SMS. Optimization of biodiesel-diesel blended fuel properties and engine performance with ether additive using statistical analysis and response surface methods. Energies 2015; 8(12): 14136-14150.

[44] Macián V, Bermúdez V, Payri R, Gimeno J. New technique for determination of internal geometry of a diesel nozzle with the use of silicone methodology. Exp Tech 2003; 27: 39-43.

[45] Hu N, Yang JG, Zhou PL, Hu Y. Study of the impact of structural parameters on the dynamic response of an electronic fuel injector. Energy Conversion and Management 2017; 136: 202-219.

[46] Binder RC. Fluid mechanics. Englewood Cliffs, New Jersey, USA: Prentice Hall; 1973.